Synthesis, Characterization and Photophysical Properties of Novel Dinuclear Silver(I) and Mononuclear Palladium(II) Complexes with 1,2-Bis[(anthracen-9-ylmethyl)amino]ethane

Guo-qi Zhang,[a] Guo-qiang Yang,*[a] Lan-ying Yang,[a] Qing-qi Chen,[b] and Jin-Shi Ma[a]

Keywords: N ligands / Palladium / Photophysics / Silver

Silver(I) (**3**) and palladium(II) (**4**) complexes of 1,2-bis[(anthracen-9-ylmethyl)amino]ethane have been synthesized and structurally characterized. X-ray crystal structure analysis reveals that compound **3** exists as a dinuclear tris(ligand) complex with formula $[Ag_2(\mathbf{2})_3]\cdot 2NO_3$, in which each silver center is three-coordinate to form a slightly distorted planar-trigonal geometry with three nitrogen donors originating from two distinct ligands. Compound **4**, on the other hand, is a mononuclear bis(ligand) complex with formula $[Pd(\mathbf{2})_2]\cdot 2OAc$, in which the palladium center is four-coordinate with four nitrogen donors originating from two distinct ligands to form a square-planar geometry. In crystals of both **3** and **4** strong intermolecular edge-to-face C–H···π packing interactions are observed, which contribute to stabilize the crystalline solid. Studies of the photophysical properties of these compounds (**3**, **4**, and ligand **2**) show apparent fluorescence quenching effect by introduction of metal ions and likely "excimer" emission of anthracene in the crystalline solid.

Introduction

Multichromophoric supramolecular architectures have been receiving increasing interest in recent years[1,2] because of their potential applications in the areas of biomedicine, molecular recognition, fluorescent sensors, and material sciences.[3–8] Anthryl and pyrenyl polyamine systems have been found to have potential uses in anion recognition, metal ion fluorescent sensors, as well as pH sensors.[9–11] Although a lot of anthryl polyamines and their metal ion complexes have been extensively investigated,[12] complexes of Ag^I and Pd^{II} are still unknown, hence it might be of considerable importance to study the structures of these complexes and correlate the structure and luminescent properties of the resultant Ag^I and Pd^{II} complexes due to the promise of polyamine systems for use as optical chemical sensors.[9] In this paper, we report the synthesis and characterization of 1,2-bis[(anthrancen-9-ylmethyl)amino]ethane (**2**) and its corresponding Ag^I complex **3** and Pd^{II} complex **4**, as well as the results of photophysical investigation on these systems.

Results and Discussion

Synthesis

The Schiff base **1** was synthesized in excellent yield by condensation of ethylenediamine with 2 equiv. of anthracene-9-carbaldehyde in DMF/MeOH at reflux. Upon treating **1** with an excess amount of $NaBH_4$ in CH_2Cl_2/MeOH at room temperature, the corresponding diamine **2** was obtained in good yield (Scheme 1). Both compounds **1** and **2** were fully characterized by combustion analysis, mass spectrometry, and ^1H and ^{13}C NMR spectroscopy.

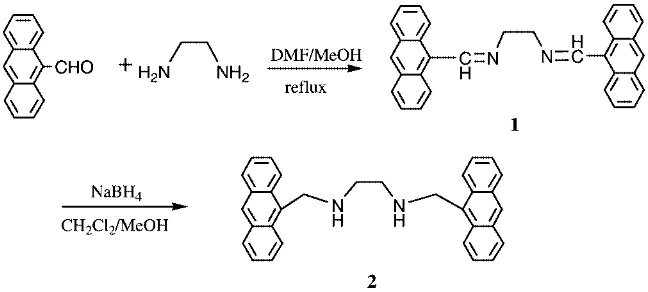

Scheme 1.

Ligand **2** was treated with silver nitrate and palladium acetate in CH_2Cl_2/MeOH (2:1, v/v) to afford the corresponding complexes **3** and **4** in yields of 70% and 64%, respectively. Crystals of **3** and **4** are reasonably stable in the mother liquors in the dark, while they slowly decompose upon exposure to light and air for a long period. Complex **4** was found to have good solubility in most polar solvents such as methanol, ethanol, dichloromethane, chloroform, acetonitrile, THF, DMF, and DMSO, while complex **3** is soluble in dichloromethane, chloroform, acetonitrile, DMF, and DMSO and slightly soluble in THF, methanol, ethanol, acetone etc.

---

[a] Center for Molecular Science, Institute of Chemistry, Chinese Academy of Sciences,
Beijing 100080, China
Fax: +86-10-8261-7315
E-mail: gqyang@iccas.ac.cn
[b] BioMarin Pharmaceutical, Inc.,
46 Galli Drive, Novato, CA 94949, USA

DOI: 10.1002/ejic.200400926

Crystal Structure of 3

The silver complex **3** crystallizes in the triclinic system with space group $P\bar{1}$. The unit cell contains two crystallographically independent dinuclear tris(ligand) complexes, three methanol molecules, and four nitrate counterions. An ORTEP drawing of the dinuclear complex cation $[Ag_2(\mathbf{2})_3]^{2+}$ is shown in Figure 1, and selected bond lengths and angles are given in Table 1. The structure consists of two Ag^I centers spanned by three ligands to form a unique dinuclear tris(ligand) complex. Each silver center is three-coordinate and adopts a slightly distorted planar-trigonal geometry with three nitrogen atoms, two of which are from one ligand, and one from the other ligand. Furthermore, two Ag atoms have almost identical coordination environments, with Ag–N bond lengths in the range 2.239(5)–2.474(5) Å. All the bond lengths are among the ranges of those found in analogous Ag^I complexes reported hitherto.[13] Moreover, the N–Ag1(A)–N bond angles of 76.6(2)° for N1(A)–Ag1(A)–N2(A), 141.4(19)° for N1(A)–Ag1(A)–N3(A), and 140.4(2)° for N2(A)–Ag1(A)–N3(A) are identical to the corresponding N–Ag1–N bond angles. In addition, two NO_3^- anions are present in the unit cell as counteranions; the Ag–O bond length is 3.761 Å, which is much longer than that of a normal Ag–O bond.[14] In the crystal of **3**, none of the anthryl moieties show intramolecular or intermolecular face-to-face π···π interactions, although significant intermolecular edge-to-face C–H···π contacts are present, and the shortest distance between an edge ring hydrogen atom and the anthracene ring center of another molecule is 2.833 Å [the angle C–H···M(mid) is 156.9°], which is in the usual range for C–H···π interactions.[15] Two adjacent molecules which show C–H···π interactions are depicted in Figure 2, where it can be seen that the C–H···π interactions serve to stabilize the crystalline solid.

Table 1. Selected bond lengths [Å] and angles [°] for complex **3**.

Ag(1)–N(3)	2.239(5)	Ag(2)–N(5)	2.338(5)
Ag(1)–N(1)	2.296(6)	Ag(2)–N(4)	2.431(6)
Ag(1)–N(2)	2.474(6)	Ag(2)–N(6)	2.234(5)
N(3)–Ag(1)–N(1)	1.44(19)	N(6)–Ag(2)–N(5)	146.19(19)
N(3)–Ag(1)–N(2)	140.4(2)	N(6)–Ag(2)–N(4)	133.94(18)
N(1)–Ag(1)–N(2)	76.6(2)	N(5)–Ag(2)–N(4)	77.6(2)
C(15)–N(1)–C(16)	109.2(6)	C(17)–N(2)–C(18)	114.8(6)
C(15)–N(1)–Ag(1)	117.3(5)	C(17)–N(2)–Ag(1)	100.4(4)
C(16)–N(1)–Ag(1)	109.2(5)	C(18)–N(2)–Ag(1)	128.9(5)
C(47)–N(3)–Ag(1)	117.2(4)	C(48)–N(3)–Ag(1)	114.2(4)

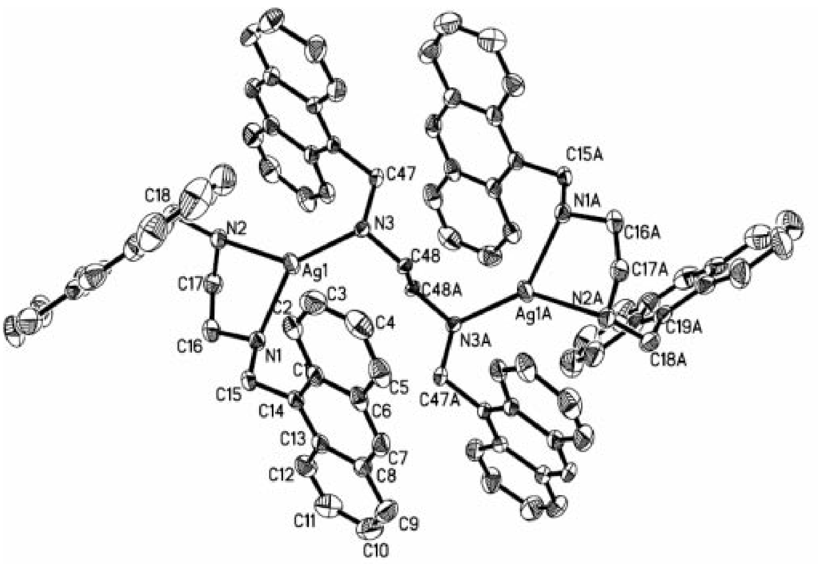

Figure 1. An ORTEP drawing of the complex cation of **3** with thermal ellipsoids at 30% probability. Hydrogen atoms, methanol, and NO_3^- counterions have been omitted for clarity.

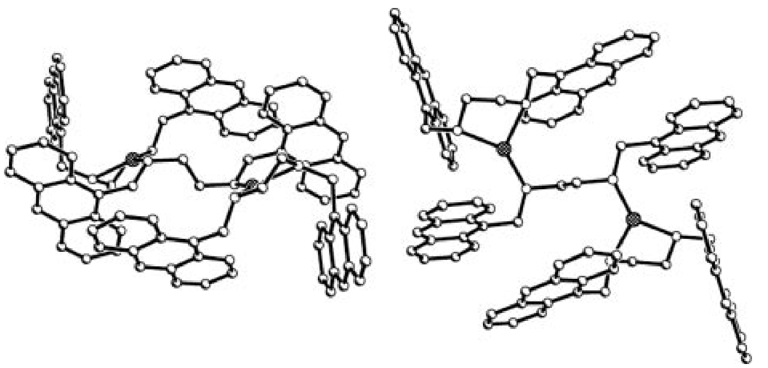

Figure 2. Two adjacent molecules in the crystal packing of **3** showing the intermolecular edge-to-face C–H···π interactions.

Crystal Structure of 4

The palladium complex **4** also crystallizes in the triclinic system with space group $P\bar{1}$. The unit cell contains seven crystallographically independent methanol molecules and two acetate anions. An ORTEP view of the mononuclear complex cation $[Pd(\mathbf{2})_2]^{2+}$ is shown in Figure 3, and selected bond lengths and angles are given in Table 2. In the crystal, the palladium center is four-coordinate to two distinct ligands to form a slightly distorted square-planar geometry. Due to the steric hindrance of the bulky anthracene group, the Pd–NH bond lengths are found to be 2.061, 2.068, 2.071, and 2.089 Å, respectively, which are slightly longer than those distances found in regular (amino)Pd^{II} (Pd–NH) complexes.[16] Interestingly, in the crystals of **4**, very strong aromatic/aromatic interactions with intermolecular edge-to-face C–H···π packing are observed [the distance between one hydrogen atom from the center ring of one anthryl unit and another molecular anthracene ring center is 2.703 Å, and the angle C–H···M(mid) is 158.1°] in contrast to **3**, which are comparable to previously reported strong C–H···π interactions (Figure 2 and Figure 4).[15]

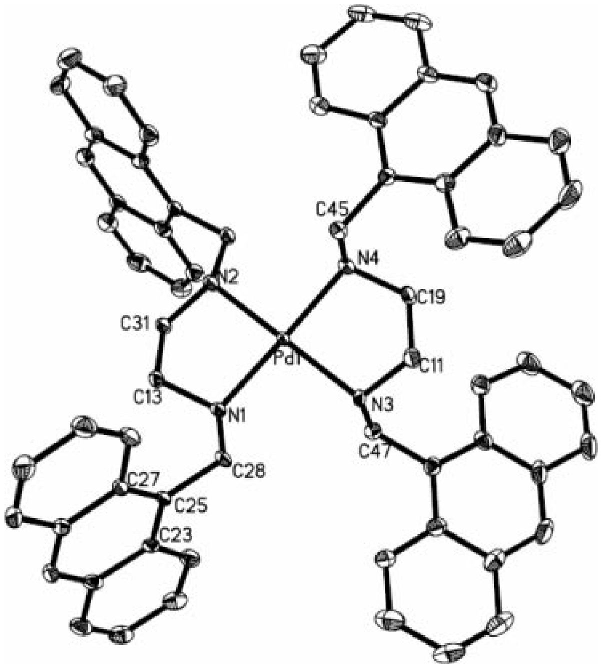

Figure 3. ORTEP view of the complex cation of **4** with thermal ellipsoids at 30% probability. Hydrogen atoms, methanol, and OAc⁻ counterions have been omitted for clarity.

Table 2. Selected bond lengths [Å] and angles [°] for complex **4**.

Pd–N(3)	2.058(5)	N(2)–C(17)	1.472(8)
Pd–N(2)	2.069(5)	N(2)–C(18)	1.512(8)
Pd–N(4)	2.060(5)	N(3)–C(49)	1.494(8)
Pd–N(1)	2.095(5)	N(3)–C(50)	1.488(7)
N(1)–C(16)	1.468(8)	N(4)–C(48)	1.502(7)
N(1)–C(15)	1.503(7)	N(4)–C(47)	1.495(7)
N(3)–Pd–N(2)	174.65(19)	C(17)–N(2)–C(18)	113.8(5)
N(3)–Pd–N(4)	84.49(19)	C(17)–N(2)–Pd	105.9(4)
N(2)–Pd–N(4)	96.0(2)	C(18)–N(2)–Pd	111.8(4)
N(3)–Pd–N(1)	95.39(19)	C(49)–N(3)–C(50)	113.0(5)
N(2)–Pd–N(1)	84.73(19)	C(49)–N(3)–Pd	106.5(3)
N(4)–Pd–N(1)	173.97(19)	C(50)–N(3)–Pd	113.7(4)
C(16)–N(1)–C(15)	114.5(5)	C(48)–N(4)–C(47)	112.2(4)
C(16)–N(1)–Pd	106.7(4)	C(48)–N(4)–Pd	105.8(3)
C(15)–N(1)–Pd	109.7(3)	C(47)–N(4)–Pd	116.1(4)

Spectroscopic and Photophysical Properties

^{1}H NMR Studies

The ^{1}H NMR spectrum of complex **3** in $CDCl_3$ shows a single set of proton resonances that can be fully assigned, which suggests that it exists as a single species in solution. Compared to the corresponding free ligand, complex **3** shows upfield shifts of 0.55–0.59 ppm for the protons of the CH_2 groups and 0.14–0.38 ppm for the protons of the anthracene rings, probably because of the intermolecular C–H···π interactions resulting from the molecular aggregation in concentrated solution, which is consistent with the case of the crystalline solid. Several attempts to measure the ^{1}H NMR spectrum of pure complex **4** in $CDCl_3$ or CD_3CN gave no satisfactory results for the signals of a single species; the spectrum shows the signals of both free ligand and a small amount of complex, which indicates that complex **4** is not very stable in solution and exists as an

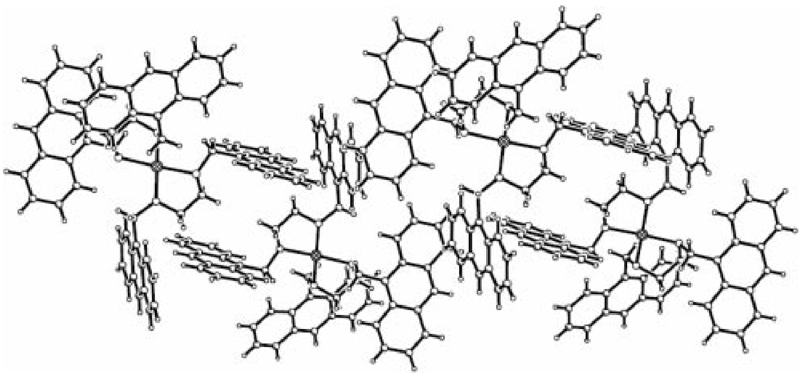

Figure 4. Packing model along the *b* axis in the crystals of complex **4** cations showing the intermolecular edge-to-face C–H···π interactions.

equilibrium between binding and disassociation due to the low binding constant of palladium ions and ligand **2**. Thus, we cannot measure the steady-state photophysics of **4** in solution, although the solid-state photoluminescence was obtained.

Photophysical Properties of 2 and 3 in Solution

The steady-state absorption and fluorescence emission spectra of **3** were measured and compared with those of the free ligand **2**. The results are reported in Table 3. The electronic absorption spectra of **2** and **3** obtained in acetonitrile at 5 μM concentration display the typical absorptions of the anthracene chromophore in the range 320–400 nm with a very slight (approximately 1–2 nm) bathochromic shift due to the introduction of silver ions (Figure 5). Moreover, in contrast to **2**, the UV/Vis spectrum of **3** shows remarkably strong absorptions at about 300 nm, which are absent in the case of the ligand as well as the silver salt under the same conditions, indicating a strong interaction between the ligand and silver ion (Figure 5).

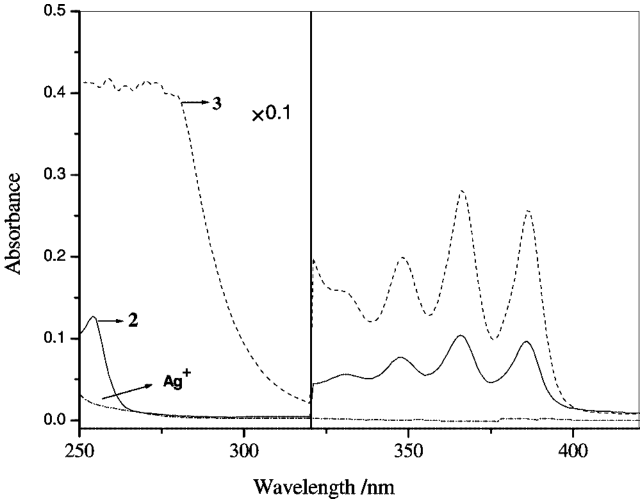

Figure 5. Electronic absorption spectra of ligand **2**, its silver complex **3**, and free Ag^+ ions in acetonitrile at room temperature (conc. 5 μM).

The fluorescence spectra of compounds **2** and **3** were recorded under the same conditions, and are given in Figure 6. The fluorescence excitation spectra were obtained by monitoring the emission at 415 nm. For **3**, except for the typical excitation spectra of the anthracene chromophore, a significantly strong excitation band in the region from 260 to 320 nm, with a maximum absorption at 293 nm, is consistent with the absorption spectra, which indicates that more efficient electronic energy transfer may take place from the metal-centered excited state to the lower energy excited state of the anthracene center.

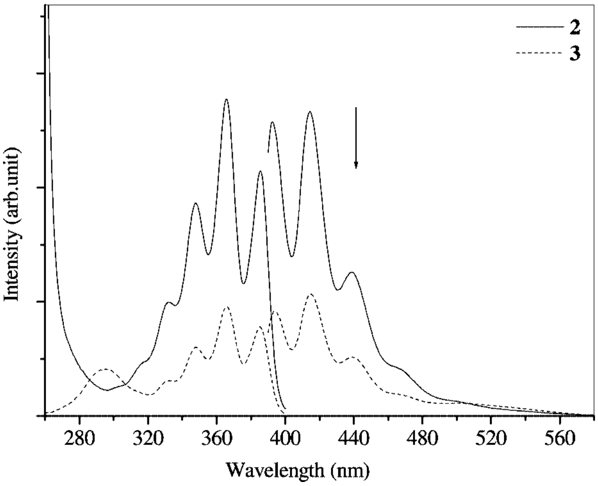

Figure 6. Fluorescence exitation (monitored at 415 nm) and emission spectra (excited at 367 nm) of **2** and **3** in acetonitrile at room temperature (conc. 5 μM).

The fluorescence intensity of the ligand **2** was found to be significantly smaller than the emission of the anthracene moiety due to a photoinduced intramolecular electron transfer (PET) process[17] from the amine lone pairs to the anthracene group, which is in agreement with previously reported anthryl or pyrenyl polyamine systems.[7,18] Upon excitation of the anthracene $S_0 \rightarrow S_1$ transition (λ_{ex} = 367 nm), emission from the anthracene chromophore is evident as a Frank–Condon vibrational process with an origin at 390 nm and a maximum intensity at 415 nm, which is in agreement with the corresponding excitation spectra. Furthermore, complex **3** displays the same quartet emission bands, in spite of the obvious difference of emission intensity. The quantum yields obtained for compounds **2** and **3** are 1.54×10^{-2} and 2.42×10^{-3}, respectively (relative to quinine sulfate in 0.1 N H_2SO_4[19]). The quantum yield of **3** is lower than that of **2**, which is indicative of a chelation-enhanced fluorescence quenching (CHEQ) effect, as reported previously for similar systems.[18] Furthermore, the measurement of fluorescence decay determines the fluorescence

Table 3. Steady-state spectroscopic data for ligand **2** and its complex **3** in CH_3CN.

Compound	Abs λ_{max} [nm]	ε_{max} ($M^{-1}cm^{-1}$)	Emission λ_{max} [nm]	Quantum yield, Φ_f	Decay times[a] τ [ns] (%)[b]	χ^2
2	366	19750	415	1.54×10^{-2}	1.3 (81.5%) 8.5 (18.5%)	1.227
3	367	56160	415	2.42×10^{-3}	1.7 (62.3%) 4.7 (37.7%)	1.193

[a] λ_{ex} = 367 nm, λ_{em} = 415 nm. [b] The percentage was obtained from: for the decay, Fit = $A + B_1 \cdot e^{(-t/\tau 1)} + B_2 \cdot e^{(-t/\tau 2)}$, $\%(\tau_1) = B_1/(B_1 + B_2)$.

decay behavior of the ligand and complex systems (see Figure 7 for the decay profiles). The fluorescence decays of both **2** and **3** were best fitted to double exponential decay processes.

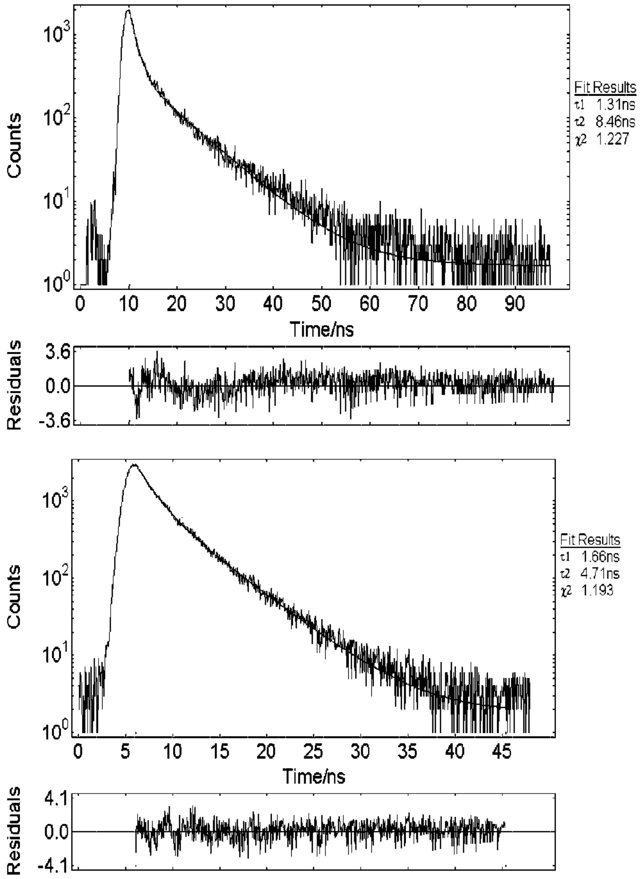

Figure 7. Fluorescence decay profiles of **2** (top) and **3** (bottom) in acetonitrile at an excitation wavelength of 367 nm. Emission monitored at 415 nm.

The transient absorption spectra of ligand **2** and its complex **3** were measured in argon-saturated acetonitrile at room temperature with concentrations of 5×10^{-4} M for **2**, and 2×10^{-4} M for **3**. The excitation wavelength generated by a nanosecond laser was 355 nm. The transient absorption spectrum of ligand **2**, depicted in Figure 8a, can be assigned to the triplet-triplet absorption (T_1-T_n absorption) of anthracene monomer based on the similarity of the spectra obtained in solutions.[20] It is known that the T_1-T_n absorption spectrum has a maximum peak at 423 nm with a molar extinction coefficient value of 64700 $M^{-1}cm^{-1}$ in cyclohexane.[20] In the given anthryldiamine compound, the transient absorption spectrum keeps the characteristic of the triplet-triplet absorption of anthracene monomer with maxima at about 400 nm and 423 nm. It decays without changing its shape and no new absorption band appears as a result of the decay, which suggests that no transient absorption of an intramolecular or intermolecular excimer occurs under these conditions. The transient absorption spectrum of complex **3** is shown in Figure 8b. No distinct absorption band appears at around 400 nm, except for a broad peak between 400 and 460 nm, and the maximum of the T_1-T_n absorption is still at about 423 nm. This may be due to the formation of new triplet species in acetonitrile from the metal-incorporated anthryldiamine **3**, although it maintains partially the characteristic of ligand **2**. In acetonitrile, the lifetime of the triplet species of ligand **2** was estimated to be 20 ± 1 μs based on the fitting to a single exponential decay curve. Obviously, a much faster triplet decay of the ligand occurs than that of triplet-state anthracene alone in solution.[20] The triplet lifetime of **3** was determined as 5.7 ± 0.1 μs with good single exponential decays, which shows that more efficient quenching occurs for the triplet species of the silver complex relative to that of the free ligand.

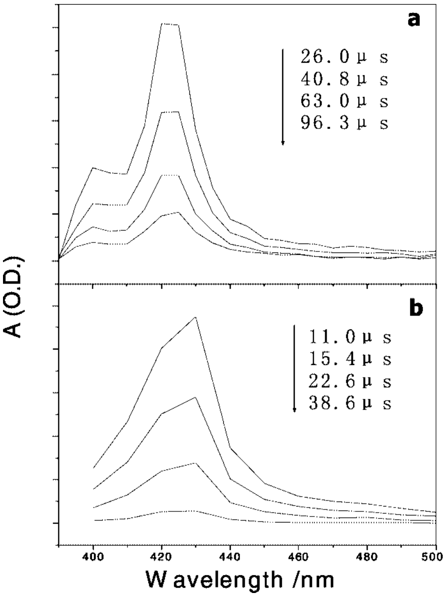

Figure 8. Transient absorption spectra of ligand **2** (a) and its silver complex **3** (b) in Ar-saturated acetonitrile at room temperature.

Photoluminescence in the Solid State

We measured the solid-state photoluminescence of both the ligand and complexes at room temperature. Although we could not measure the photophysical properties of complex **4** in solution due to its instability, the measurement of the solid-state photoluminescence is still helpful for understanding the emission behavior of the complex. More significantly, the solid-state spectra usually exhibit the features of the aggregated state of molecules in combination with the crystal structure in the solid state. Obviously, both the free ligand and complexes are photoluminescent in the solid state (Figure 9) when excited at 366 nm. However, the emission position is remarkably bathochromic relative to that in solution, which may be attributed to the increased intermolecular interaction as a result of closer packing of the molecules in the solid state, and, interestingly, both the ligand and complexes display emission even in the longer wavelength range (>500 nm), which is possibly attributed to an "excimer" emission of anthracene[21,22] reminiscent of the structural characterization of the two complexes depicted above. The obviously weak emission of **4** in the solid state may be due to a CHEQ effect similar to the situation of **3** in solution.

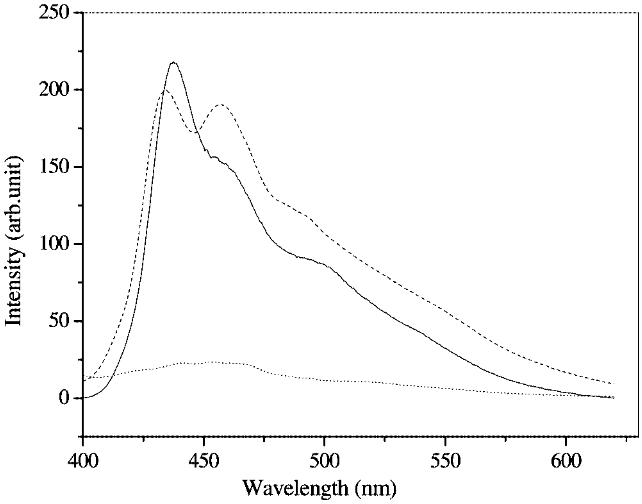

Figure 9. Solid-state photoluminescence spectra of **2** (solid), **3** (dot), and **4** (dash) at room temperature.

Conclusions

In summary, we have synthesized a new anthryldiamine ligand **2** as well as the corresponding silver complex **3** and palladium complex **4**. In the solid state, complex **3** forms a dinuclear tris(ligand) supramolecular architecture, while **4** is a mononuclear bis(ligand) complex. The preferential coordination in these complexes matches the requirements of the steric hindrance of the bulky ligands and the nature of the metal ions. Significantly strong intermolecular edge-to-face C–H···π packing interactions are observed in crystals of both **3** and **4**, which contribute to stabilize the crystalline solid. Complex **3** is very stable while **4** partially disassociates in solution due to its low binding constant. Photophysical studies have shown that the PET process is present in ligand **2** and an efficient CHEQ effect is also observed for its metal complexes. The transient absorption spectra allowed us to determine the absorption features and decay lifetimes of the triplet species of **2** and **3**. The solid-state photoluminescence studies showed the bathochromic emission relative to that in solution and likely "excimer" emission of anthracene in the crystalline solid, thereby indicating the presence of intermolecular interactions, in agreement with the results of ^{1}H NMR studies and the crystal-structure analysis.

Experimental Section

Materials and General Methods: All the reagents were commercially available. Anthracene-9-carbaldehyde, ethylenediamine, sodium borohydride, silver nitrate, and palladium acetate were used without further purification. Solvents for syntheses were purified according to standard methods, while those for spectral measurements were purchased as spectrophotometric grade. Samples for C, H, N analyses were dried under vacuum and the analyses were performed with a Carlo Erba-1106 Instrument. ^{1}H NMR spectra were measured with a Bruker dmx 300 MHz NMR spectrometer at room temperature in $CDCl_3$ with tetramethylsilane as the internal reference. The ESI and MALDI-TOF MS measurements were carried out with a Bruker APEX II instrument. UV/Vis absorption spectra were obtained with a Hitachi UV-3010 absorption spectrophotometer. Steady-state excitation and emission spectra were recorded with a Hitachi F-2500 fluorescence spectrophotometer. Fluorescence lifetime was detected at 415 nm with a fluorescence lifetime analytical spectrometer (Erdinburgh FLS-920) and the samples were excited at 367 nm (maximum absorption wavelength). Time-resolved transient absorption spectra were measured with an Edinburgh LP920 nanosecond flash photolysis instrument.

1,2-Bis[(anthracen-9-ylmethylene)amino]ethane (1): Anthracene-9-carbaldehyde (9.5 g, 46.1 mmol) was dissolved in 120 mL of DMF/MeOH (1:5, v/v), and then heated at reflux. A solution of ethylenediamine (1.6 mL, 23.0 mmol) in 10 mL of methanol was added dropwise to this mixture with vigorous stirring. A yellow precipitate appeared after a few minutes, and the mixture was refluxed for an additional 4 h. Upon cooling, the yellow precipitate was separated by filtration under reduced pressure, then washed with a few drops of DMF and a large volume of methanol. The product was recrystallized from CH_3OH/CH_2Cl_2 to give yellow plates. Yield: 9.2 g (92%), m.p. 229–230°C. ^{1}H NMR (300 MHz, $CDCl_3$, 25°C, TMS): δ = 4.52 (s, 4 H, CH_2), 7.11 (dd, J = 7.8, J = 7.8 Hz, 4 H, anthryl-H), 7.36 (dd, J = 7.8, J = 7.2 Hz, 4 H, anthryl-H), 7.96 (d, J = 8.4 Hz, 4 H, anthryl-H), 8.41 (s, 2 H, anthryl-H), 8.45 (d, J = 7.2 Hz, 4 H, anthryl-H), 9.50 (s, 2 H, imine-H) ppm. ^{13}C NMR (75 Hz, $CDCl_3$): δ = 31.0, 63.1, 125.0, 125.2, 126.5, 128.6, 129.3, 130.0, 131.2, 162.4 ppm. MALDI-TOF-MS: m/z = 436 [M$^+$]. $C_{32}H_{24}N_2$ (436.2): calcd. C 88.04, H 5.54, N 6.42; found C 87.58, H 5.56, N 6.29.

1,2-Bis[(anthracen-9-ylmethyl)amino]ethane (2): $NaBH_4$ (1.3 g) was dissolved in 10 mL of anhydrous methanol and then added in small portions to a suspension of **1** (1.3 g, 3 mmol) in 150 mL of CH_2Cl_2/MeOH (2:1, v/v) at 50 °C under N_2 over 2 h. The mixture turned gradually to a clear yellowish color and the resulting solution was allowed to react at room temperature overnight. The solvent was then removed under reduced pressure and the residue was treated with excess water. The insoluble materials were then collected by suction, and recrystallized twice from CH_2Cl_2 to give light-yellow needles. Yield: 0.9 g, 68%, m.p. 185–186 °C. ^{1}H NMR (300 MHz, $CDCl_3$, 25°C TMS): δ = 3.07 (s, 4 H, CH_2), 4.72 (s, 4 H, CH_2), 7.44 (m, 8 H, anthryl-H), 8.00 (d, J = 6.0 Hz, 4 H, anthryl-H), 8.29 (d, J = 7.89 Hz, 4 H, anthryl-H), 8.40 (s, 2 H, anthryl-H) ppm. ^{13}C NMR (75 Hz, $CDCl_3$): δ = 45.5, 49.6, 124.0, 124.8, 126.0, 127.1, 129.0, 130.1, 131.4 ppm. MALDI-TOF-MS: m/z = 440 [M$^+$]. $C_{32}H_{28}N_2\cdot 1/4H_2O$ (444.7): calcd. C 86.28, H 6.40, N 6.29; found C 86.30, H 6.41, N 6.20.

Ag^{I} Complex 3: A solution of **2** (132 mg, 0.3 mmol) in CH_2Cl_2 (20 mL) was slowly added to 10 mL of a methanolic solution of $AgNO_3$ (25.5 mg, 0.15 mmol). The resulting colorless solution was stirred at room temperature for 30 min and then filtered. The clear filtrate was allowed to stand in the dark at room temperature, and after about two weeks colorless block-like single crystals suitable for X-ray analysis were collected by filtration. An analytical sample was dried under vacuum to remove the solvents. Yield: 87 mg (70%) based on $AgNO_3$. M.p. 161–162 °C. ^{1}H NMR (300 MHz,

$CDCl_3$, 25°C TMS): δ = 2.52 (s, 12 H, CH_2), 4.13 (s, 12 H, CH_2), 7.27–7.33 (m, 24 H, anthryl-H), 7.74 (d, J = 8.1 Hz, 12 H, anthryl-H), 7.91 (d, J = 7.89 Hz, 12 H, anthryl-H), 8.08 (s, 6 H, anthryl-H) ppm. MALDI-TOF-MS: m/z = 767.4 $[M - 2\ NO_3]^{2+}$. $C_{96}H_{84}Ag_2N_2 \cdot 2NO_3 \cdot CH_3OH$ (1690.5): calcd. C 68.79, H 5.24, N 6.62; found C 68.91, H 5.24, N, 6.65.

Pd^{II} Complex 4: Complex **4** was prepared by a procedure similar to that of **3**. A solution of **2** (132 mg, 0.3 mmol) in CH_2Cl_2 (20 mL) was slowly added to 10 mL of a methanolic solution of $Pd(OAc)_2$ (33.7 mg, 0.15 mmol). The resulting orange solution was stirred at room temperature for 30 min and then filtered. The clear filtrate was allowed to stand at 5 °C, and after about one week, light-orange, block-like single crystals suitable for X-ray analysis were obtained. An analytical sample was dried under vacuum. Yield: 101 mg, 64%; M.p. 119–121 °C. ESI-MS: m/z = 985.5 $[M - 2\ OAc - H]^+$. $C_{64}H_{68}N_4Pd \cdot 2OAc \cdot CH_3OH \cdot H_2O$ (1154.4): calcd. C 71.71, H 5.93, N 4.85; found C 71.30, H 5.60, N 4.73.

X-ray Crystallography: Crystals suitable for X-ray diffraction studies were obtained by slow evaporation of the solvents from CH_2Cl_2/MeOH solutions. Accurate unit-cell parameters were determined by a least-squares fit of 2θ values measured for 200 strong reflections. Intensity data sets were measured with a Bruker Smart 1000 CCD or Rigarku Raxis Rapid IP diffractometer with Mo-K_α radiation (λ = 0.71073 Å) at room temperature. The intensities were corrected for Lorentz and polarization effects, but no corrections for extinction were made. All structures were solved by direct methods. The non-hydrogen atoms were located in successive difference Fourier syntheses. The final refinement was performed by full-matrix least-squares methods with anisotropic thermal parameters for non-hydrogen atoms on F^2. The hydrogen atoms were added theoretically as riding on the appropriate atoms. Crystallographic data and experimental details for structure analyses are summarized in Table 4. CCDC-230566 (**3**) and -230567 (**4**) contain the supplementary crystallographic data for this paper. These data can be obtained free of charge from The Cambridge Crystallographic Data Centre via www.ccdc.cam.ac.uk/data_request/cif.

Table 4. Crystallographic data for complexes **3** and **4**.

	3	**4**
Empirical formula	$C_{96}H_{84}Ag_2N_8O_6$	$C_{75}H_{83}N_4O_{11}Pd$
Formula mass	1658.46	1322.85
Color	colorless	pale yellow
Crystal system	triclinic	triclinic
Space group	$P\bar{1}$	$P\bar{1}$
T [K]	293(2)	293(2)
λ [Å]	0.71073	0.71073
a [Å]	14.497(7)	12.978(3)
b [Å]	16.595(9)	14.094(3)
c [Å]	17.707(9)	18.590(4)
α [°]	85.859(9)	80.59(3)
β [°]	77.817(8)	84.13(3)
γ [°]	75.575(8)	84.23(3)
V [Å^3]	4032(4)	3324.7(11)
Z	4	2
F(000)	1770	1390
ρ_{calc} [gcm^{-3}]	1.408	1.321
Goodness-of-fit on F^2	1.021	0.998
μ [mm^{-1}]	0.551	0.344
$R^{[a]}$	0.0625	0.0778
$wR2^{[b]}$	0.1449	0.2066

[a] $R = \Sigma(F_o - F_c)/\Sigma(F_o)$. [b] $wR2 = \Sigma w(F_o{}^2 - F_c{}^2)^2/\Sigma w(F_o{}^2)^2]^{1/2}$.

Acknowledgments

This work was financially supported by NSFC (50221201) and the major state basic research development program (G2000078100) of China.

---

[1] a) J.-M. Lehn, *Supramolecular Chemistry*, Wiley-VCH, Weinheim, **1995**; b) V. Balzani, F. Scandola, *Supramolecular Photochemistry*, Ellis Horwood, New York, **1991**; c) M. R. Wasielewski, *Chem. Rev.* **1992**, *92*, 435–461; d) K. S. Schanze, D. B. Macqueen, T. A. Perkins, L. A. Cabana, *Coord. Chem. Rev.* **1993**, *122*, 63–89.

[2] J.-E. Sohna, P. Jaumier, F. Fages, *J. Chem. Res. (S)* **1999**, 134–135.

[3] a) S. Boyde, G. F. Strouse, W. E. Jones, T. J. Meryer, *J. Am. Chem. Soc.* **1989**, *111*, 7448–7454; b) S. L. Mecklenburg, K. A. Opperman, P. Chen, T. J. Meryer, *J. Phys. Chem.* **1996**, *100*, 15 145–15 151 and references cited therein.

[4] a) G. J. Wilson, A. Launikonis, W. H. F. Sasse, A. W. H. Mau, *J. Phys. Chem. A* **1997**, *101*, 4860–4866; b) W. E. Ford, M. A. J. Rodgers, *J. Phys. Chem.* **1992**, *96*, 2917–2920.

[5] a) P. Belser, R. Dux, M. Baak, L. De Cola, V. Balzani, *Angew. Chem. Int. Ed. Engl.* **1995**, *34*, 595–598; b) D. R. McDonald, R. J. Crutchley, *Inorg. Chem.* **1994**, *33*, 1899–1906; c) J. Otsuki, N. Okuda, T. Amamiya, K. Araki, M. Seno, *Chem. Commun.* **1997**, 311–312.

[6] B. Bodenant, F. Fages, M. H. Delville, *J. Am. Chem. Soc.* **1998**, *120*, 7511–7519.

[7] R. Martínez-Máñez, F. Sancenón, *Chem. Rev.* **2003**, *103*, 4419–4476 and references cited therein.

[8] M. E. Huston, E. U. Akkaya, A. W. Czarnik, *J. Am. Chem. Soc.* **1989**, *111*, 8735–8737.

[9] a) G. De Santis, L. Fabbrizzi, M. Licchelli, A. Poggi, A. Taglietti, *Angew. Chem. Int. Ed. Engl.* **1996**, *35*, 202–204; b) L. Fabbrizzi, I. Faravelli, G. Francese, M. Licchelli, A. Perotti, A. Taglietti, *Chem. Commun.* **1998**, 971–972; c) L. Fabbrizzi, M. Licchelli, A. Perrotti, A. Poggi, G. Rabaioli, A. Taglietti, *J. Chem. Soc., Perkin Trans. 2* **2001**, 2108–2113; d) L. Fabbrizzi, M. Licchelli, F. Mancin, M. Pizzeghello, G. Rabaioli, A. Taglietti, P. Tecilla, U. Tonellato, *Chem. Eur. J.* **2002**, *8*, 94–101; e) F. Sancenón, A. Benito, J. M. Lloris, R. Martínez-Máñez, T. Pardo, J. Soto, *Helv. Chim. Acta* **2002**, *85*, 1505–1516; f) S. A. Van Arman, A. W. Czarnik, *J. Am. Chem. Soc.* **1990**, *112*, 5376–5377; g) S.-Y. Hong, A. W. Czarnik, *J. Am. Chem. Soc.* **1993**, *115*, 3330–3331.

[10] a) S. A. McFarland, N. S. Finney, *J. Am. Chem. Soc.* **2001**, *123*, 1260–1261; b) J. Kang, M. Choi, J. Y. Kwon, E. Y. Lee, J. Yoon, *J. Org. Chem.* **2002**, *67*, 4384–4386.

[11] a) P. Schwab, M. Levin, J. Michl, *Chem. Rev.* **1999**, *99*, 1863–1934; b) P. V. Bernhardt, E. G. Moore, M. J. Riley, *Inorg. Chem.* **2001**, *40*, 5799–5805; c) P. V. Bernhardt, G. A. Lawrance, T. W. Hambley, *J. Chem. Soc., Dalton Trans.* **1989**, 1059–1066; d) P. V. Bernhardt, E. G. Moore, M. J. Riley, *Inorg. Chem.* **2002**, *41*, 3025–3031; e) F. DeRosa, X. Bu, P. C. Ford, *Inorg. Chem.* **2003**, *42*, 4171–4178; f) M. A. Bernado, F. Pina, E. García-España, J. Latorre, S. V. Luis, J. M. Llinares, J. A. Ramírez, C. Soriano, *Inorg. Chem.* **1998**, *37*, 3935–3942.

[12] a) V. Balzani, M. Juris, M. Venturi, S. Campagna, S. Serrioni, *Chem. Rev.* **1996**, *96*, 759–834; b) J. E. Moser, P. Bonnôte, M. Grätzel, *Coord. Chem. Rev.* **1998**, *171*, 245–250; c) V. Balzani, M. Gómez-López, J. F. Stoddart, *Acc. Chem. Res.* **1998**, *31*, 405–414; d) R. Ballardini, V. Balzani, A. Credi, M. T. Gandolfi, M. Venturi, *Acc. Chem. Res.* **2001**, *34*, 445–455; e) D. Pomeranc, V. Heitz, J.-C. Chambron, J.-P. Sauvage, *J. Am. Chem. Soc.* **2001**, *123*, 12 215–12 221; f) G. Benkö, J. Kallioonen, J. E. I. Korppi-Tommola, A. P. Yartsev, V. Sundström, *J. Am. Chem. Soc.* **2002**, *124*, 489–493.

[13] a) X.-H. Bu, H. Liu, M. Du, K. M.-C. Wong, V. W.-W. Yam, M. Shionoya, *Inorg. Chem.* **2001**, *40*, 4143–4149; b) M. Hong,

W. Su, R. Cao, M. Fujita, J. Lu, *Chem. Eur. J.* **2000**, *6*, 427–431; c) H. Arii, Y. Saito, Y. Funahashi, T. Ozawa, K. Jitsukawa, H. Masuda, *Eur. J. Inorg. Chem.* **2003**, 2917–2919.

[14] a) M.-L. Tong, X.-M. Chen, B.-H. Ye, L.-N. Ji, *Angew. Chem. Int. Ed.* **1999**, *38*, 2237–2240; b) B. S. Fox, M. K. Beyer, V. E. Bondybey, *J. Am. Chem. Soc.* **2002**, *124*, 13 613–13 623; c) I. Ino, L. P. Wu, M. Munakata, M. Maekawa, Y. Suenaga, T. Kuroda-Sowa, Y. Kitamori, *Inorg. Chem.* **2000**, *39*, 2146–2151.

[15] T. Steiner, *Angew. Chem. Int. Ed.* **2002**, *41*, 48–76 and references cited therein.

[16] a) R. Ahlrichs, M. Ballauff, K. Eichkorn, O. Hanemann, G. Kettenbach, P. Klüfers, *Chem. Eur. J.* **1998**, *4*, 835–844; b) K. Haas, E. M. Ethrenstorfer-Scäfers, K. Polnorn, W. Beck, *Eur. J. Inorg. Chem.* **1999**, 465–469.

[17] A. P. De Silva, R. A. D. D. Rupasinghe, *J. Chem. Soc., Chem. Commun.* **1985**, 1669–1670.

[18] a) J. A. Sclafani, M. T. Maranto, T. M. Sisk, S. A. Van Arman, *Tetrahedron Lett.* **1996**, *37*, 2193–2196; b) J. Yoon, N. E. Ohler, D. H. Vance, W. D. Aumiller, A. W. Czarnik, *Tetrahedron Lett.* **1997**, *38*, 3845–3848; c) F. Pina, M. A. Bernardo, E. Garcia-Espana, *Eur. J. Inorg. Chem.* **2000**, 2143–2157; d) F. Sancenón, A. B. Descalzo, J. M. Lloris, R. Martínez-Máñez, T. Pardo, M. J. Seguí, J. Soto, *Polyhedron* **2002**, *21*, 1397–1404.

[19] J. N. Demas, G. A. Crosby, *J. Phys. Chem.* **1971**, *75*, 991–1024.

[20] a) R. Bensasson, E. Land, *Trans. Faraday Soc.* **1971**, *67*, 1904–1915; b) K. Kikuchi, *Triplet-Triplet Absorption Spectra*, Bunshin Publishing, Tokyo, **1989**.

[21] a) T. Hayashi, N. Mataga, Y. Sakata, S. Misumi, N. Morita, J. Tanaka, *J. Am. Chem. Soc.* **1976**, *98*, 5910–5913; b) J. K. McVey, D. M. Shold, N. C. Yang, *J. Chem. Phys.* **1976**, *65*, 3375–3376; c) W. L. Jorgensen, D. L. Severance, *J. Am. Chem. Soc.* **1990**, *112*, 4768–4774; d) D. A. Evans, K. T. Chapman, D. T. Hung, A. T. Kawaguchi, *Angew. Chem. Int. Ed. Engl.* **1987**, *26*, 1184–1186 and references cited therein.

[22] a) I. Y. Chan, H. Ismail, B. Prass, D. Stehlik, *J. Chem. Phys.* **2002**, *117*, 4419–4427; b) Z. Fei, N. Kocher, C. J. Mohrschladt, H. Ihmels, D. Stalke, *Angew. Chem. Int. Ed.* **2003**, *42*, 783–787.

Received: November 3, 2004